



# Gas-phase H<sub>2</sub> absorption and microstructural properties of LaNi<sub>5-x</sub>Ge<sub>x</sub> alloys

C. Witham\*, R.C. Bowman Jr., B. Fultz

*Division of Engineering and Applied Science, California Institute of Technology, Pasadena, 91125 California USA*

## Abstract

Metal hydride alloys were prepared based on the LaNi<sub>5</sub> formula by substituting 0–10 at.% of Ge for Ni. Crystal lattice parameters were obtained from X-ray diffraction patterns of each alloy. Hydrogen pressure–composition–temperature isotherms were measured for these LaNi<sub>5-x</sub>Ge<sub>x</sub> (0 ≤ x ≤ 0.5) alloys at temperatures ranging 296 to 348 K. These isotherms were used to determine thermodynamic parameters for hydrogen absorption and desorption. The unit cell volumes increase, and the plateau pressures decrease, with increasing Ge substitution. Isotherms and capacities from gas-phase absorption are comparable to those of LaNi<sub>5-x</sub>Sn<sub>x</sub>.

*Keywords:* Metal hydrides; Pressure–composition–temperature isotherm; Hydrogen storage alloys; LaNi<sub>5-x</sub>Ge<sub>x</sub>H system; Thermodynamics; Hysteresis

## 1. Introduction

The prevailing methodology for changing the hydriding properties of LaNi<sub>5</sub> is to substitute different metals for Ni or La. Properties that can be affected include absorption and desorption pressures, hysteresis, capacity, enthalpies and entropies of hydride phase formation and decomposition, and cyclic lifetimes under both gas-phase and electrochemical cycling [1]. Luo et al. published measurements of many of these properties in alloys that had systematically increasing amounts of Sn substituted for Ni [2]. Mendelsohn et al. [3] briefly identified Ge as a substituent for Ni, but no further work was done. Recently, we used Ge as a substituent for Ni in alloys employed in Ni-MH cells [4]. Ge does not lower the plateau pressure of the alloy as much as Sn, but affects its capacity comparably and may make the alloy more stable against corrosion in an alkaline medium.

In this paper we give a more complete characterization of Ge-substituted LaNi<sub>5</sub>. We have characterized the microstructure with X-ray diffractometry (XRD) and electron microprobe analysis. The thermodynamic parameters for the formation and decomposition of the hydride phase in LaNi<sub>5-x</sub>Ge<sub>x</sub>H<sub>y</sub> were determined by measuring pressure–composition–temperature isotherms at temperatures ranging from 296 K to 348 K. Because Ge and Sn are both 4-valent s-p metals, and are similar in Mendeleev number,

[5] the properties of LaNi<sub>5-x</sub>Ge<sub>x</sub> are compared to those of LaNi<sub>5-x</sub>Sn<sub>x</sub>.

## 2. Experimental

Stoichiometric amounts of La (99.99%), Ni (99.99%), and Ge (99.99%) from Johnson Matthey were alloyed in an induction melting furnace and annealed in argon at 950°C for 72 h. Isotherm measurements were made with an automated Sievert's apparatus constructed at Caltech. ULSI hydrogen (99.9999%) gas from Matheson Gas Products was used for the isotherm studies. All gas handling equipment was constructed using 316 stainless steel components, and the MH alloy was contained in a double-walled copper reactor designed to enhance thermal conductivity [6]. The ingots were activated by a single hydrogen absorption–desorption cycle before isotherm measurements.

Isotherms were measured at 296, 323, and 348 K. Elevated temperature isotherms were obtained in a constant temperature water bath. The alloys were heated to about 513 K after each isotherm and were evacuated to 10<sup>-4</sup> torr by a Tribodyn oil-free molecular drag vacuum pump. Chemical composition analyses of the annealed alloy ingots were performed with a JEOL Superprobe 733 electron microprobe. Phase fractions and unit cell lattice parameters were measured in powders that had undergone

\*Corresponding author.

isotherm measurements with an INEL CPS-120 powder diffractometer using Co K $\alpha$  radiation ( $\lambda=1.7902$  Å).

### 3. Results

#### 3.1. XRD

Fig. 1 shows the XRD patterns of the  $\text{LaNi}_{5-x}\text{Ge}_x$  alloys,  $0 \leq x \leq 0.5$ . All compositions but  $x=0.5$  yield single phase materials with the  $\text{CaCu}_5$  crystal structure (Haucke phase). This was confirmed by microprobe analysis, which revealed a few percent of equiaxed precipitates of approximately  $\text{LaNiGe}$  composition in a Haucke phase matrix in the  $x=0.5$  sample. Lattice parameters were extracted by a Nelson–Riley extrapolation to determine the dehydrided unit cell volumes. The anisotropic peak broadening resulting from hydrogen activation complicates the fitting of overlapping peaks. To compensate for this, only peaks whose  $l$  index is less than the sum of  $h$  and  $k$  indexes were used to determine the  $a$  parameter, and peaks whose  $l$  index is greater than or equal to the sum of  $h$  and  $k$  indexes were used for the  $c$  parameter. The increase in the unit cell volume upon substitution is approximately linear with Ge composition,  $x$ , as shown in Fig. 2.

#### 3.2. Isotherms

Room temperature isotherms of all Ge substituted alloys are compared in Fig. 3 to that of  $\text{LaNi}_5$ . It can be seen that both the absorption and desorption plateau pressures and the hydrogen absorption capacities decrease with Ge substitution. Fig. 3 also shows that the hysteresis between

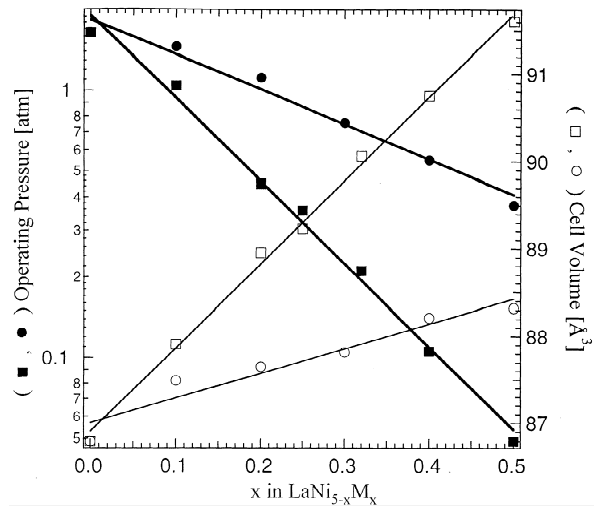


Fig. 2. Correlation of  $\text{LaNi}_{5-x}\text{M}_x$  plateau pressures (filled) and unit cell (open) volumes with  $x$ ,  $\text{M}=\text{Sn}$  (square symbol) or  $\text{Ge}$  (circular symbol).

the absorption and desorption isotherms is decreased with increasing Ge composition. The hysteresis ratios of the room temperature hydride formation and decomposition plateau pressures at mid-plateau have been calculated using the expression:

$$RT/2 \ln(P_a/P_d), \quad (1)$$

and are shown in Table 1.

Elevated temperature isotherms were measured for all alloys, and examples are presented in Fig. 4 for  $\text{LaNi}_{4.7}\text{Ge}_{0.3}$ . The pressures at mid-plateau are used in van't Hoff plots (Fig. 5) to calculate the enthalpy and

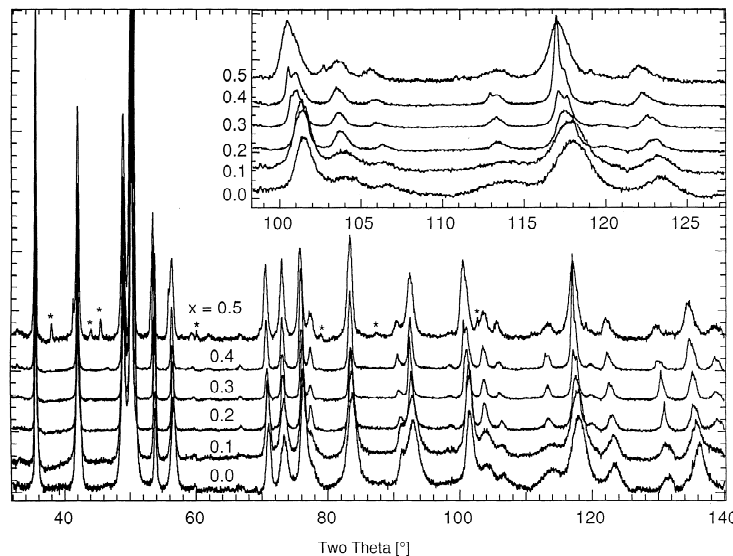


Fig. 1. X-ray diffraction patterns of  $\text{LaNi}_{5-x}\text{Ge}_x$  for  $0 \leq x \leq 0.5$ ,  $x$  shown in graph. The symbols (\*) denote peaks from secondary phases in  $\text{LaNi}_{4.5}\text{Ge}_{0.5}$ .

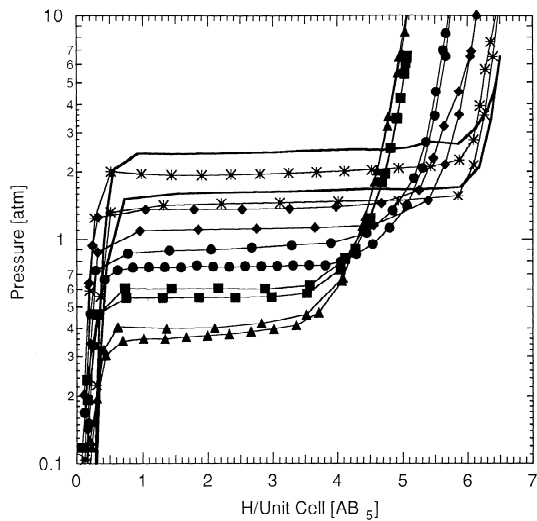


Fig. 3. Room temperature (23°C) gas-phase isotherms of (\*)  $\text{LaNi}_{4.9}\text{Ge}_{0.1}$ , ( $\blacklozenge$ )  $\text{LaNi}_{4.8}\text{Ge}_{0.2}$ , ( $\bullet$ )  $\text{LaNi}_{4.7}\text{Ge}_{0.3}$ , ( $\blacksquare$ )  $\text{LaNi}_{4.6}\text{Ge}_{0.4}$ , ( $\blacktriangle$ )  $\text{LaNi}_{4.5}\text{Ge}_{0.5}$  alloys, and gas-atomized (-)  $\text{LaNi}_5$  alloy.

entropy of hydride formation and decomposition, which are presented in Table 1. The isotherm and thermodynamic data for  $x=0.4$  agree well with the values reported by Mendelsohn et al. [3]. We see that in all cases the enthalpy of hydride decomposition is higher in magnitude than that of formation. The absolute enthalpy also decreases with increasing Ge composition. Both of these points are consistent with the decrease in isotherm plateau pressure. The entropy calculations show a somewhat less consistent trend of an increase in absolute entropy with increasing Ge composition.

### 3.3. Reversible hydrogen storage capacity

The reversible gas-phase hydrogen storage capacity was determined by calculating the width of the room temperature isotherms to 2 atm, and is shown in Table 1. The plateau width is not decreased severely for  $x < 0.4$ .

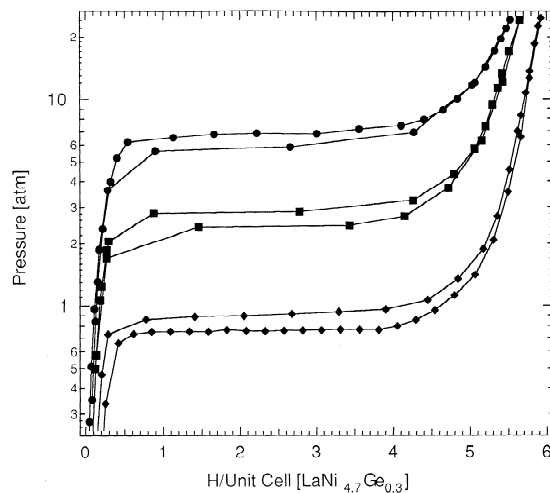


Fig. 4. Elevated temperature gas-phase isotherms of  $\text{LaNi}_{4.7}\text{Ge}_{0.3}$ : ( $\blacklozenge$ ) 296 K, ( $\blacksquare$ ) 323 K, and ( $\bullet$ ) 348 K.

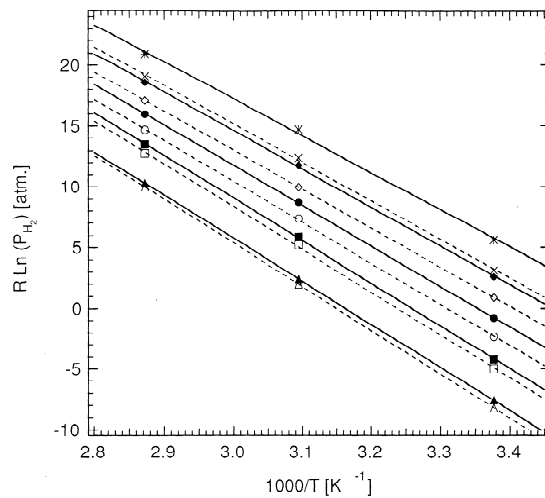


Fig. 5. Van't Hoff plots of (\*)  $\text{LaNi}_{4.9}\text{Ge}_{0.1}$ , ( $\blacklozenge$ )  $\text{LaNi}_{4.8}\text{Ge}_{0.2}$ , ( $\bullet$ )  $\text{LaNi}_{4.7}\text{Ge}_{0.3}$ , ( $\blacksquare$ )  $\text{LaNi}_{4.6}\text{Ge}_{0.4}$ , ( $\blacktriangle$ )  $\text{LaNi}_{4.5}\text{Ge}_{0.5}$  alloys. Open symbols denote absorption isotherms, and closed symbols denote desorption isotherms.

Table 1  
Thermodynamic and hydriding parameters of  $\text{LaNi}_{5-x}\text{Ge}_x$ .

Alloy	Unit cell volume ( $\text{\AA}^3$ )	$(\text{H}/\text{M})_{\text{max}}^{\text{a}}$	23°C $P_{\text{H}_2}^{\text{b}}$ (atm)		$ \Delta\text{H} $ (kJ/mol H)		$ \Delta\text{S} $ (J/K/mol H)		Hysteresis ratio <sup>d</sup> (J/mol H)
			abs	des	abs	des	abs	des	
$\text{LaNi}_5$	86.80	6.45	2.48	1.65		15.4 <sup>c</sup>		53.9 <sup>c</sup>	502
$\text{LaNi}_{4.9}\text{Ge}_{0.1}$	87.49	6.25	1.96	1.46	15.2	15.8	54.2	55.1	368
$\text{LaNi}_{4.8}\text{Ge}_{0.2}$	87.65	5.95	1.37	1.11	15.8	16.1	54.8	54.6	254
$\text{LaNi}_{4.7}\text{Ge}_{0.3}$	87.82	5.60	0.906	0.755	16.6	16.9	55.8	55.8	226
$\text{LaNi}_{4.6}\text{Ge}_{0.4}$	88.21	5.00	0.603	0.548	17.6	17.6	57.2	57.0	118
	87.8 <sup>e</sup>		0.85 <sup>e,f</sup>	0.78 <sup>e,f</sup>		17.2		55.4	109 <sup>c</sup>
$\text{LaNi}_{4.5}\text{Ge}_{0.5}$	88.32	4.90	0.400	0.372	17.7	18.0	56.1	56.7	92

<sup>a</sup> Isotherm measured to 2 atm; <sup>b</sup> Measured at middle of plateau; <sup>c</sup> Taken from Ref. [9]; <sup>d</sup>  $RT/2 \ln(P_{\text{a}}/P_{\text{d}})$  (at 23°C); <sup>e</sup> Taken from Ref. [3]; <sup>f</sup> Isotherm taken at 30°C.

#### 4. Discussion

The metallic radius of Sn is 26% larger than that of Ni, whereas Ge is 10% larger than Ni [7]. It is therefore expected that Sn substitution for Ni will cause an expansion of the unit cell of  $\text{LaNi}_5$  by a greater amount than will the substitution of Ge for Sn, provided that Ge and Sn both occupy the same Ni site in the unit cell. This is in fact the trend obtained from linear fits of the cell volumes,  $V_{\text{Sn}}$  and  $V_{\text{Ge}}$ , versus solute composition. Expressing the solute concentration as  $x$  in the formulae  $\text{LaNi}_{5-x}\text{Sn}_x$  and  $\text{LaNi}_{5-x}\text{Ge}_x$  we found (in units of  $\text{\AA}^3$ ):

$$V_{\text{Ge}} = 87.006 + 2.84x, \quad V_{\text{Sn}} = 86.908 + 9.58x. \quad (2a,b)$$

From Fig. 2 we see that the logarithm of the plateau pressure correlates linearly to the unit cell volume of the material. This trend is consistent with correlations reported previously for solute substituted  $\text{LaNi}_5$  alloys [8].

The slopes of our van't Hoff diagrams were reliable, so we expect that the enthalpies reported in Table 1 are accurate. The trends for the enthalpy of hydrogen absorption and desorption are correlated to the unit cell volumes as:

$$H_{\text{abs}} = 247.5 - 3.0041V_{\text{Ge}},$$

$$H_{\text{des}} = 214.1 - 2.6277V_{\text{Ge}}, \quad (3)$$

confirming the linear relationship seen by previous researchers [8].

Since the isotherms were obtained over a relatively narrow range of temperature, our values for the entropy are probably less reliable. Nevertheless, agreement with values reported from previous studies on substituted  $\text{AB}_5$  MH alloys [2,3,9] encourages us that the measurements are qualitatively accurate. The anomalous decrease in entropy for the alloy with  $x_{\text{Ge}} = 0.5$  may be caused by the presence of the second phase that was found in this material. The compositional trend for the entropy of hydrogen absorption correlates with the widths of the plateau shown in Fig. 3 [10].

Because the hysteresis ratios were calculated from isotherms measured after only one gas-phase activation, they are expected to be larger than steady-state values [11]. Nevertheless, we believe that there is a strong decrease in the hysteresis ratio with increasing Ge substitution for Ni. The effect of Sn on the hysteresis ratio has been reported to be larger, however [2].

Fig. 6 shows a side-by-side comparison of gas-phase isotherms from  $\text{LaNi}_{5-x}\text{Ge}_x$  and  $\text{LaNi}_{5-x}\text{Sn}_x$ ,  $0 \leq x \leq 0.5$ . The scales of the pressure axes are different by an order of magnitude. The hysteresis is therefore not consistent in the two graphs, as can be seen by examining the isotherm of the binary alloy (dashed line). The compositional trends in plateau pressures reflect the trends in enthalpies for hydrogen absorption in the two alloy systems, both related

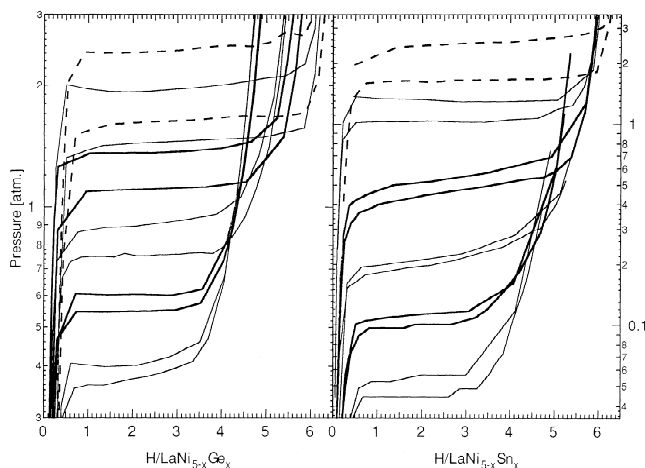


Fig. 6. Comparison of room temperature gas-phase isotherms of  $\text{LaNi}_{5-x}\text{Sn}_x$  and  $\text{LaNi}_{5-x}\text{Ge}_x$  with scaled pressure axes. Dashed line— $\text{LaNi}_5$ ,  $x$  progression indicated by alternating thin and thick lines

logarithmically to the unit cell volume. More surprising are the similarities in width and shapes of the isotherms. The elements Ge and Sn, which have similar thermochemical properties [5], cause similar effects on the hydriding behavior of  $\text{LaNi}_5$ . In a preliminary report,  $\text{LaNi}_{5-x}\text{Ge}_x$  alloys were shown to have good cycle lifetimes in nickel-metal hydride batteries [4]. The possibility for large amounts of Ge substitution seems promising for developing battery electrodes with good electrochemical capacity retention during the charge-discharge cycling.

#### 5. Conclusions

We have prepared a series of alloys of composition  $\text{LaNi}_{5-x}\text{Ge}_x$ , where  $0 \leq x \leq 0.5$ . X-ray diffractometry showed that the alloys were single phase with the  $\text{CaCu}_5$  crystal structure for  $x < 0.5$ , and the unit cell was expanded for alloys with increasing Ge content. We measured gas-phase isotherms on all these alloys and found that Ge suppresses the absorption plateau, decreases the hysteresis, and has only a modest effect in reducing the width of the plateau. The  $\text{LaNi}_{5-x}\text{Ge}_x$  alloys show compositional trends for hydrogen absorption similar to those of  $\text{LaNi}_{5-x}\text{Sn}_x$ , although more Ge than Sn is needed to attain the same plateau pressure. Large Ge substitutions may be possible in  $\text{LaNi}_{5-x}\text{Ge}_x$  alloys for service in nickel-metal hydride batteries, and this is encouraging because preliminary reports are that Ge substitution offers improvements in the cycle lifetimes of battery electrodes.

#### Acknowledgments

The authors thank Prof. Ted Flanagan (U. Vermont) for providing his isotherm data on the annealed  $\text{LaNi}_{5-x}\text{Sn}_x$

alloys. This work was carried out at the California Institute of Technology under funding by the DOE grant DE-FG03-94ER14493.

## References

- [1] A. Percheron-Guegan, M. Lacroche, J.C. Achard, Y. Chabre and J. Bouet, in P.D. Bennett and T. Sakai (eds.), *Hydrogen and Metal Hydride Batteries, PV 94-27*, The Electrochemical Society Proceedings Series, Pennington, NJ, 1994, p. 196.
- [2] S. Luo, W. Luo, J.D. Clewley, Ted B. Flanagan and L.A. Wade, *J. Alloys Comp.*, 231 (1995) 467.
- [3] M. Mendelsohn, D. Gruen and A. Dwight, *Inorg. Chem.*, 18 (1979) 3343.
- [4] C. Witham, B.V. Ratnakumar, R.C. Bowman Jr., A. Hightower and B. Fultz, *J. Electrochem. Soc.*, 143 (1996) L205.
- [5] D.G. Pettifor, *Mater. Sci. Technol.*, 4 (1988) 2480.
- [6] R.C. Bowman Jr., C.H. Luo, C.C. Ahn, C.K. Witham and B. Fultz, *J. Alloys Comp.*, 217 (1995) 185.
- [7] E.T. Teatum, K.A. Gschneider Jr. and J.T. Waber, *Compilation of Calculated Data Useful in Predicting Metallurgical Behavior of the Elements in Binary Alloy Systems*, Los Alamos Laboratory Report LA-4003, 1968.
- [8] A. Percheron-Guegan, J.C. Achard, J. Sarradin and G. Bronoël, in A.F. Andresen and A.J. Maeland (eds.), *Hydrides for Energy Storage*, Pergamon Press, Oxford, 1978, p. 485.
- [9] G. Sandrock, P. Goodell, E. Huston and P. Golben, *Z. Phys. Chem. N.F.*, 164 (1989) 1285.
- [10] D.M. Gruen and M. Mendelsohn, *J. Less-Comm. Metals*, 55 (1977) 149.
- [11] K. Nomura, H. Uruno, S. Ono, H. Shinozuka and S. Suda, *J.*